COLLECTIVE TRANSVERSE INSTABILITIES IN THE GSI SYNCHROTRONS: DAMPING INDUCED BY INTERNAL AND/OR EXTERNAL NONLINEARITIES

V. Kornilov, O. Boine-Frankenheim and I. Hofmann
GSI Darmstadt, Planckstr. 1, 64291 Darmstadt, Germany

Abstract

Collective instabilities are a potential limiting factor for the performance of the FAIR [1] rings at GSI Darmstadt. We discuss results of experimental and numerical investigations of transverse collective beam behavior in the SIS 18 synchrotron. Damping mechanisms in the presence of space charge, especially Landau damping and decoherence due to nonlinearities are discussed; effects induced by internal-only, external-only nonlinearities, and combinations of the both are addressed. As a computational tool accounting the beam nonlinear dynamics with impedances and self-consistent space charge, the particle tracking code `PATRIC` is used.

INTRODUCTION

During dedicated experiments at SIS 18 with a high intensity (5e10 particles) Ar_{40}^{18+} coasting beam at the injection energy (11.4 MeV/u) on March 15, 2006, robust transverse collective instabilities have beam observed. Figure 1 displays the time evolution of the vertical position for the beam center (the upper one) and of the beam current (bottom) and demonstrates the increase of coherent perturbation (with the growth time approx. 20 ms), its saturation and the simultaneous beam loss. The observed dipole oscillation is at 160 kHz, the frequency of the slow-wave mode $n = 4$ (which should be the most unstable one for the resistive-wall exciting mechanism) and set tune $Q_{\mathrm{vert}} = 3.29$ is f_{rw} =154 kHz. The difference might have resulted from a deviation of the actual tune. With the growth time in a good agreement with the impedance estimation, we conclude that this is the resistive-wall instability.

Space charge effects are crucial for SIS–synchrotrons due to weakly-relativistic velocities and small beam aperture/radius ratios. Landau damping mechanisms should become effective to damp the instabilities. For example, for the SIS 18 beam at the injection energy the coherent frequency lies fairly close to the incoherent spread, where the linear Landau damping (due to the momentum spread) can have an effect. Other damping mechanisms, as due to nonlinearities (amplitude-dependent incoherent tune) may then become decisive for FAIR rings.

Nonlinear Landau damping influences the collective beam motion due to an incoherent tune spread, which can be induced by internal effects (nonlinear space charge) and by external nonlinearities (e.g., an octupole). Additionally, there exists a complex interplay between the two nonlinear damping mechanisms. Although a number of analytical works have been done (e.g., [2]-[5]), there is still some uncertainty about questions as (a) whether damping due to internal nonlinearity effects alone is effective; (b) how damping mechanisms interfere for the combination of external and internal nonlinearities; etc. Our strategy in this work is to try to further clarify the issue by solving two different dispersion relations and performing simulations using the code `PATRIC`. We consider the most interesting cases (internal effects alone, external nonlinearity alone, combination of both) for identical beam parameters and compare results.

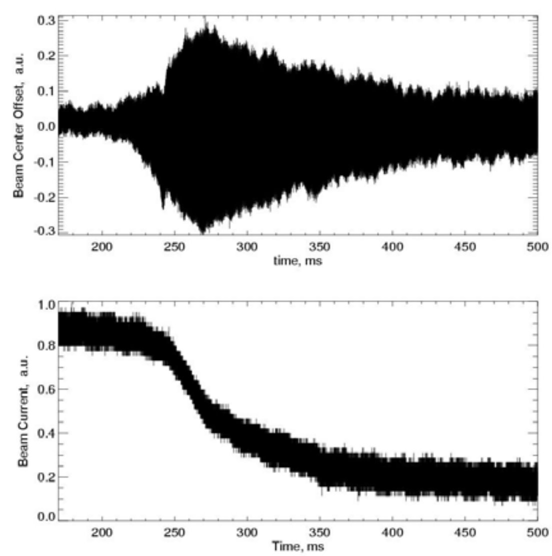

Figure 1: The transverse collective instability measured in SIS 18. Top: beam position, bottom: beam current.

TWO DISPERSION RELATIONS

Two different analytic approaches to describe damping due to nonlinearities can be found in the literature.

The first approach [2] formulates the dispersion relation,

$$A\,Z^{\perp}(\Omega) = \left[-i \int \frac{\mathrm{d}\psi_0}{\mathrm{d}a} \frac{a\mathrm{d}a}{\Omega/\omega_0 - Q(a)} \right]^{-1}, \qquad (1)$$

where $\psi_0(a)$ is the stationary part of the amplitude distribution, Ω is the complex collective frequency to be found, $(AZ^{\perp})$ is the normalized transverse dipole impedance

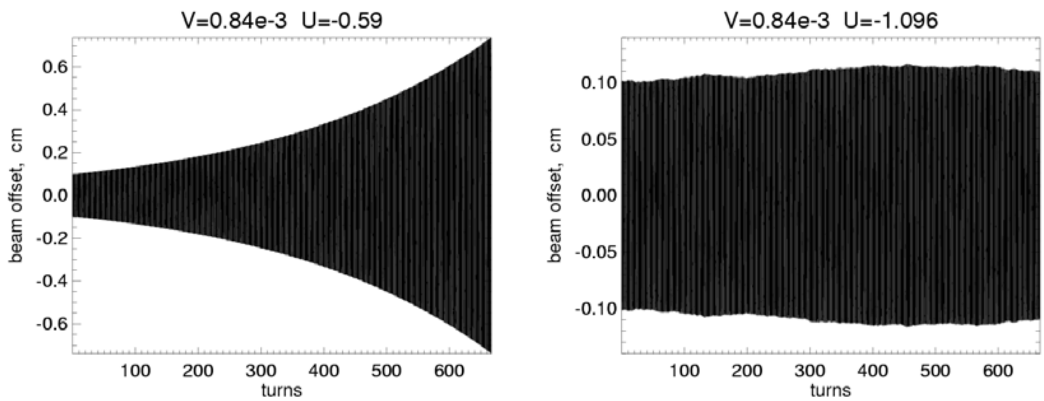

Figure 2: Typical time evolutions of the beam center from simulations using PATRIC for two different $\mathcal{I}m(Z^{\perp})$; left: no damping (instability); right: damping dominates (stable). Normalized impedances V, U correspond to Fig. 3, right.

which includes coherent and incoherent interactions, and $Q(a)$ is the complete incoherent particle tune.

Within the second approach [3] one constructs another dispersion relation,

$$\int \frac{\mathrm{d}\psi_0}{\mathrm{d}a} \frac{[\Delta Q_{\mathrm{coh}} - \Delta Q_{\mathrm{inc}}(a)]a\mathrm{d}a}{\Omega/\omega_0 - (Q_0 + \Delta Q_{\mathrm{inc}})} = 1 \ , \tag{2}$$

where ΔQ_{coh} is the coherent tune shift (i.e., $\propto Z^{\perp}_{\mathrm{coh}}$), $Q_0(a)$ includes only tune shifts due to external nonlinearities and $\Delta Q_{\mathrm{inc}}(a)$ is the tune shift induced by internal effects only (here, nonlinear space-charge).

The decisive difference between these two approaches is the way how tune shifts are treated. Eq. (1) does not separate explicitly contributions to tune shifts induced by external and internal forces. This leads to a damping (the integral has a singularity) whenever the coherent tune overlaps the incoherent tune spread. In contrast, the second approach [Eq. (2)] treats separately the nonlinearities of different nature. In a situation without external effects (when Q_0 is the bare tune) the integral in Eq. (2) has no pole which means the solution Ω is real. Thus Eq. (2) predicts no damping for this case even if the coherent tune overlaps the incoherent tune spectrum.

Solution of the dispersion relations

Both of the dispersion relations Eq. (1) and Eq. (2), which are formulated in a simplified manner here, we solve numerically. The amplitude-dependent tune shift due to nonlinear space-charge is integrated numerically. Including the cubic component of the transverse force from an octupole lens, the tune shift of the classical anharmonic oscillator is taken into account, $\Delta Q^{\mathrm{oct}}(a) \propto K_3 a^2$, where $K_3 = \frac{1}{B\rho}\frac{\mathrm{d}^3 B_y}{\mathrm{d}x^3}$ is the octupole strength for the horizontal motion. The waterbag distribution is assumed for the beam and the integration is performed one-dimensionally for the horizontal plane.

PARTICLE TRACKING SIMULATIONS

For simulations of instabilities and nonlinear dynamics in accelerator rings we employ the particle-in-cell tracking code PATRIC, which is a part of the numerical development effort in the High-Current-Beam-Physics group at GSI Darmstadt. Particle are moved in a complete 3D and nonlinear description. For the space charge, the sliced approach (”$2\frac{1}{2}$–dimension“) with self-consistent electric field is used. Two solvers for the Poisson equation are implemented, for rectangular and elliptic boundary conditions. Transfer matrix calculated by the code MADX can be used. The impedance implementation allows to model an arbitrary external (coherent) impedance spectra.

Parameters for the simulations presented here were chosen in a way to achieve the closest possible condition to that used for the dispersion relations. The beams were matched in size, a constant focusing model was used for the lattice. In simulations with external nonlinearities, a cubic component (characterized by the octupole coefficient K_3), distributed along the ring, was super-imposed onto the particle motion. As an initial condition, the waterbag distribution was chosen. In the simulations, presented here, we did not observe noticeable modifications of the particle distribution, other types of the beam distribution were not examined for this work. To focus on the physics of nonlinearities, we exclude effects of the finite momentum spread. A round pipe as boundary condition has been used. Note that other types of a conducting wall, as elliptic or rectangular one, produce external incoherent tune shifts and for this reason they are inapplicable for the case of internal effects only.

Series of simulations have been performed with varying both $\mathcal{R}e(Z^{\perp})$ and $\mathcal{I}m(Z^{\perp})$ to study comprehensively the stability properties. Change of $\mathcal{I}m(Z^{\perp})$ shifts proportionally the coherent frequency Ω and allows to scan it over the incoherent spectrum (the coherent shift from the image charges of the conducting wall must then be taken into account). SIS 18–similar costing beam parameters have been assumed, with the factor 5 larger intensity to make

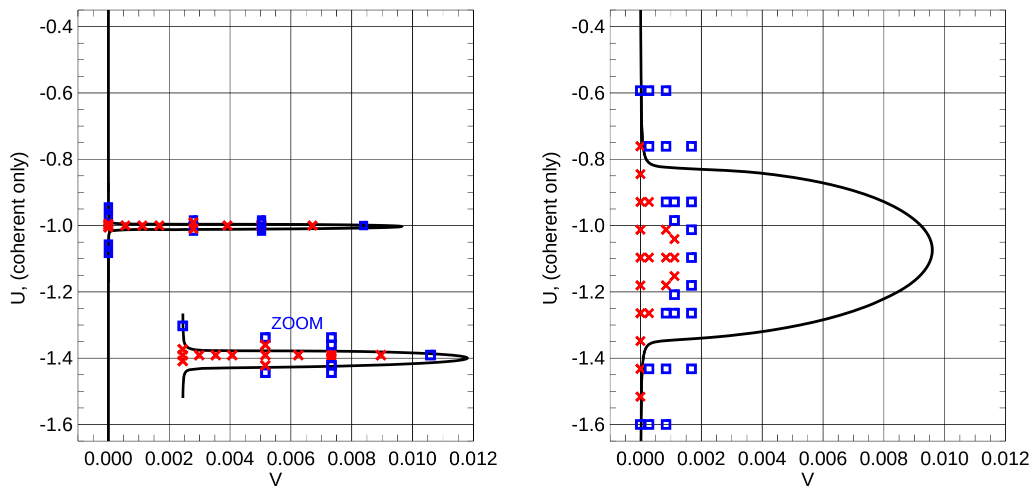

Figure 3: Comparison of results of simulations (□ and ×, see the previous figure for examples) with solution of the dispersion relation Eq. (2) (lines). Left: external nonlinearity alone, right: combination of external and internal (nonlinear space-charge) nonlinearities. $V \propto \mathcal{R}e(Z^{\perp})$; $U \propto \mathcal{I}m(Z^{\perp}) \propto \Delta\Omega_{\rm coh}$.

growth- and damping times smaller for reasonable computing times. A rather weak external nonlinearity (octupole $K_3 = 5\,{\rm m}^{-4}$) was assumed to keep the beam distribution regular. Small enough initial perturbations were used. As an example, Fig. 2 shows the characteristic behavior of the beam center simulated for fixed finite $\mathcal{R}e(Z^{\perp})$ but different $\mathcal{I}m(Z^{\perp})$. Without incoherent tune spread, both of these beams would be identically unstable. Here, the case of the combination of nonlinear space-charge and octupole effects is taken.

For the results presented here we used an octupole with a polarity, which shifts the incoherent tune in the same direction as space charge. Thus it enhances the internal-effect tune spread. With the opposite polarity, the octupole acts as a reduction, which we do not discuss here due to shortage of space.

COMPARISONS AND DISCUSSION

Our first trilateral comparison is for the case of internal-effects-alone, where dispersion relations Eq. (1) and Eq. (2) provide the largest qualitative discrepancy. Series of simulations with the code `PATRIC` for zero and finite $\mathcal{R}e(Z^{\perp})$ and extensive $\mathcal{I}m(Z^{\perp})$–scans did not show any damping, which supports the prediction of the dispersion relation Eq. (2) [3].

Next, we solve the dispersion relation Eq. (2) for the external-nonlinearity-alone case (Fig. 3, left) and for the combination of both nonlinearities (Fig. 3, right). The lines in Fig. 3 show the stability boundaries, i.e., the contour level for $\mathcal{I}m(\Omega) = 0$ in the normalized coherent impedance plane $V + iU = AZ^{\perp}$. The stable areas lie on the left of these lines. V is proportional to the resistive impedance, U to $\mathcal{I}m(Z^{\perp})$ and to the coherent frequency shift $\Delta\Omega$; the normalization is such that $U = \Delta\Omega/|\Delta\omega_{\rm dsc}|$, where $\Delta\omega_{\rm dsc}$ is the incoherent direct space-charge shift of the equivalent flat-profile beam. According to Eq. (2), an addition of the nonlinear space-charge effect to the external nonlinearity results in a strong enhancement of the stability, whereas the size of the stable area remains unchanged in $\mathcal{R}e(Z^{\perp})$ and greatly enlarges in $\mathcal{I}m(Z^{\perp})$ (see Fig. 3).

Results of simulations scans are also shown in Fig. 3 with squares (no damping, as Fig. 2, left) and crosses (damping dominates, as Fig. 2, right), where each of these symbols is an outcome of a simulation run. In the case of external nonlinearity alone (Fig. 3, left) there is an agreement between Eq. (2) and `PATRIC` simulations. For the combinations of nonlinearities (Fig. 3, right) our simulations confirm the enlargement of the stability along $\mathcal{I}m(Z^{\perp})$, but they disagree with the dispersion relation regarding the extent of the stability area in $\mathcal{R}e(Z^{\perp})$. Our simulations predict a significant reduction of the instability threshold in $\mathcal{R}e(Z^{\perp})$ for the combinations of nonlinearities with respect to the damping induced by external nonlinearities alone. Reasons for the discrepancy may be connected with the facts that the dispersion relation Eq. (2) is a one-dimensional approximation of the 2D problem and the approach of Ref. [3] is based on heuristic argumentation.

REFERENCES

[1] P. Spiller, these proceedings

[2] J. Laclare, Proc. Symp. on Accel. Aspects of heavy ion Fusion, GSI-82-8, p. 278 (1982)

[3] D. Möhl, H. Schönauer, Proc. IX Int. Conf. High Energy Acc., Stanford, 1974, p. 380 (1974)

[4] E. Métral, F. Ruggiero, Proc. EPAC2004, Lucerne, Switzerland, 5-9 July 2004, p. 1897 (2004)

[5] M. Blaskiewicz, Phys. Rev. ST Accel. Beams **4**, 044202 (2001)